Theoretical Study of Light Refraction in Three-Dimensional Photonic Crystals

Xiaonan Chen, Wei Jiang, *Member, IEEE*, Jiaqi Chen, and Ray T. Chen, *Fellow, IEEE*

***Abstract*—A rigorous theory for solving general 3-D photonic crystal refraction problem is developed. The power flow direction and transmission intensity of each mode refracted at a periodic surface are rigorously analyzed and determined from matrix equations. We further illustrate how to apply our method to design a low-index-contrast 3-D superprism structure that exhibits efficient transmission over a wide angular scanning range at wavelengths near 1550 nm.**

***Index Terms*—Light refraction, superprism, 3-D photonic crystals (PCs), transmission.**

I. Introduction

ANOMALOUS light refraction, or the superprism effect, has been experimentally demonstrated in 3-D photonic crystal (PC) structures, which are fabricated through a self-organization method [1]. Proposed applications for the superprism effect include wavelength demultiplexing [1], 3-D integrated photonics circuits that are based on self-collimation propagation [2], sensing and filtering [3], and 3-D functional superlenses that are based on subwavelength imaging [4]. The refraction angle and transmission intensity of each propagating mode inside the PC are two intrinsic optical properties we must investigate before fabrication. A powerful physical concept for studying light beam directions is the PC dispersion surface, which is commonly calculated using the conventional plane wave expansion (PWE) method [5]. For transmission, the popular finite-difference time-domain technique is often time consuming, particularly for large-volume 3-D structure simulations. Li and Ho introduced a PWE-based transfer-matrix method (TMM) to study the transmitted field amplitude through a single PC surface [6]. Jiang *et al.* developed the first rigorous theory to analyze light refraction and transmission by a 2-D PC having a general lattice type and an arbitrary surface orientation that includes both an ordinary Miller-indexed surface and a quasi-periodic surface [7]. However, a general PC refraction theory that can efficiently and reliably predict transmission and reflectivity for light refraction in 3-D PCs is rarely seen in the literature. In this paper, we will present a full-vectorial refraction theory for electromagnetic (EM) wave propagation in semi-infinite 3-D PC structures in Section II. Furthermore, we will discuss, in detail, how to employ our theory to design and simulate a 3-D PC superprism structure with efficient transmission modes in Section III.

Manuscript received February 7, 2007; revised May 21, 2007. This work was supported by a polymer nanophotonics program funded by Air Force Research Laboratory.

X. Chen, J. Chen, and R. T. Chen are with the Microelectronics Research Center, University of Texas at Austin, Austin, TX 78758 USA (e-mail: xiaonan_chen@mail.utexas.edu; jchen83@mail.utexas.edu; raychen@uts.cc.utexas.edu).

W. Jiang is with the Microelectronics Research Center, University of Texas at Austin, Austin, TX 78758 USA, and also with the Omega Optics, Austin, TX 78758 USA (e-mail: jiang@ece.utexas.edu).

Digital Object Identifier 10.1109/JLT.2007.902753

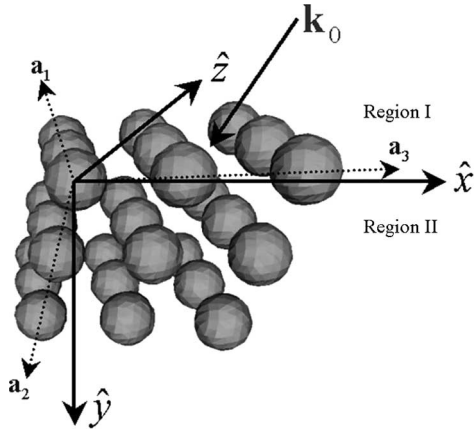

Fig. 1. General schematic of a 3-D PC structure.

II. Description of the Theory

A general schematic of a 3-D PC structure is depicted in Fig. 1; a unit cell with PC dielectric function $\varepsilon(\mathbf{x})$ replicates periodically along three independent directions $\mathbf{a}_1$, $\mathbf{a}_2$, and $\mathbf{a}_3$. A planar wave $e^{i\mathbf{k}_0\mathbf{x}}$ with frequency ω is incident upon the interface, which is defined as an $x-z$ plane, between a uniform medium and a PC region. For convenience, we sometimes refer to the uniform medium region $(y<0)$ as region I and the PC region $(y>0)$ as region II. Consider the equivalent transform of Maxwell equations

$$\begin{cases} i\omega\mu_0\mathbf{H} = \nabla\times\mathbf{E} \\ -i\omega\varepsilon_0\varepsilon(\mathbf{x})\mathbf{E} = \nabla\times\mathbf{H} \end{cases}. \tag{1}$$

By substitution for E_y and H_y, we may obtain the linear equations with reduced field variables

$$\begin{cases} \omega^2\mu_0\varepsilon_0\begin{bmatrix} H_x \\ H_z \end{bmatrix} = i\omega\varepsilon_0\frac{\partial}{\partial y}\begin{bmatrix} -E_z \\ E_x \end{bmatrix} + \begin{bmatrix} -\partial/\partial z \\ \partial/\partial x \end{bmatrix} \\ \qquad\qquad \times\left[\frac{1}{\varepsilon(\mathbf{x})}\left(\frac{\partial H_x}{\partial z}-\frac{\partial H_z}{\partial x}\right)\right] \\ \omega^2\mu_0\varepsilon_0\begin{bmatrix} E_x \\ E_z \end{bmatrix} = \frac{i\omega\mu_0}{\varepsilon(\mathbf{x})}\frac{\partial}{\partial y}\begin{bmatrix} H_z \\ -H_x \end{bmatrix} + \frac{1}{\varepsilon(\mathbf{x})} \\ \qquad\qquad \times\begin{bmatrix} -\partial/\partial z \\ \partial/\partial x \end{bmatrix}\left(\frac{\partial E_x}{\partial z}-\frac{\partial E_z}{\partial x}\right) \end{cases}. \tag{2}$$

In the PC region, the field equations may be expressed with a Fourier expansion in terms of Fourier coefficients

$$\begin{aligned}
&\omega^2\mu_0\varepsilon_0 H_x(\mathbf{G}) \\
&\quad = \omega\varepsilon_0(k_y+G_y)E_z(\mathbf{G}) + \sum_{\mathbf{G_1}}(k_z+G_z)\eta(\mathbf{G}-\mathbf{G_1}) \\
&\qquad \times[(k_z+G_{1z})H_x(\mathbf{G_1}) - (k_x+G_{1x})H_z(\mathbf{G_1})] \\
&\omega^2\mu_0\varepsilon_0 H_z(\mathbf{G}) \\
&\quad = -\omega\varepsilon_0(k_y+G_y)E_x(\mathbf{G}) - \sum_{\mathbf{G_1}}(k_x+G_x)\eta(\mathbf{G}-\mathbf{G_1}) \\
&\qquad \times[(k_z+G_{1z})H_x(\mathbf{G_1}) - (k_x+G_{1x})H_z(\mathbf{G_1})] \\
&\omega^2\mu_0\varepsilon_0 E_x(\mathbf{G}) \\
&\quad = -\omega\mu_0\sum_{\mathbf{G_1}}(k_y+G_{1y})\eta(\mathbf{G}-\mathbf{G_1})H_z(\mathbf{G_1}) \\
&\qquad + \sum_{\mathbf{G_1}}(k_z+G_{1z})\eta(\mathbf{G}-\mathbf{G_1}) \\
&\qquad \times[(k_z+G_{1z})E_x(\mathbf{G_1}) - (k_x+G_{1x})E_z(\mathbf{G_1})] \\
&\omega^2\mu_0\varepsilon_0 E_z(\mathbf{G}) \\
&\quad = \omega\mu_0\sum_{\mathbf{G_1}}(k_y+G_{1y})\eta(\mathbf{G}-\mathbf{G_1})H_x(\mathbf{G_1}) \\
&\qquad - \sum_{\mathbf{G_1}}(k_x+G_{1x})\eta(\mathbf{G}-\mathbf{G_1}) \\
&\qquad \times[(k_z+G_{1z})E_x(\mathbf{G_1}) - (k_x+G_{1x})E_z(\mathbf{G_1})] \quad (3)
\end{aligned}$$

where $\mathbf{G}$ is a reciprocal lattice vector, which is given by $\mathbf{G}_{lmn} = l\mathbf{b}_1 + m\mathbf{b}_2 + n\mathbf{b}_3$, $-L \le l \le L$, $-M \le m \le M$, $-N \le n \le N$. Here, L, M, and N denote the truncations of the Fourier series in three dimensions. $\mathbf{b}_1$, $\mathbf{b}_2$, and $\mathbf{b}_3$ are the basis vectors of the reciprocal lattice. For a semi-infinite PC structure with a periodic surface, a set of "primitive" translation vectors can always be chosen to keep $\mathbf{b}_2$ along the $\hat{y}$ axis if the surface is periodic [7], [8]. The Fourier coefficient $\eta_{\mathbf{G}} = V^{-1}\int_{\text{cell}} d^3\mathbf{x}\cdot e^{-i\mathbf{G}\cdot\mathbf{x}}\varepsilon^{-1}(\mathbf{x})$, where V is the volume of a unit cell. $E(\mathbf{G})$ and $H(\mathbf{G})$ are the Fourier coefficients of EM fields, respectively. The tangential components k_x and k_z may be obtained by matching boundary conditions at the $y = 0$ plane.

Consider the matrix form of (3), $[\mathbf{K}][\mathbf{F}] = k_y[\mathbf{W}][\mathbf{F}]$, where the elements of matrices $[\mathbf{K}]$ and $[\mathbf{W}]$ are functions of ω, k_x, k_z, and ε. The solutions of the matrix equation are given by $\det([\mathbf{W}]^{-1}[\mathbf{K}] - k_y\mathbf{I}) = 0$, where $\mathbf{I}$ is an identity matrix, and k_y is the eigenvalue of $[\mathbf{W}]^{-1}[\mathbf{K}]$. The column vector $[\mathbf{F}]$ is composed of four subcolumn vectors, $[E_x(\mathbf{G}_{lmn})]$, $[E_z(\mathbf{G}_{lmn})]$, $[H_x(\mathbf{G}_{lmn})]$, and $[H_z(\mathbf{G}_{lmn})]$, which are given by the eigenvector solutions of $[\mathbf{W}]^{-1}[\mathbf{K}]$. The Fourier coefficients of E_y and H_y may be further solved from the substitution equations. The total number of the eigenvalues is $R = 4(2L+1)(2M+1)(2N+1)$, since both $[\mathbf{K}]$ and $[\mathbf{W}]$ are $R \times R$ square matrices. In each conjugate pair of the complex k_y roots, $\text{Im}(k_y) < 0$ results in divergence such that only $\text{Im}(k_y) > 0$ is allowed inside the PC region. Real k_y can be partitioned into an equal number of forward- and backward- propagating modes, since half of the real k_y modes have a positive y component of the Poynting vector [7]. In addition, all $k_y^{(m)} = k_y + mb_2$, $m = -M, -M+1, \ldots, M$ may degenerate into one distinct solution due to the periodicity of the Brillouin zones [7]. Therefore, the independent mode number is further reduced to $2(2L+1)(2N+1)$ due to degeneracy [7].

The next step is to evaluate the properties of each distinct mode. The time-independent Poynting vector may be calculated by $\mathbf{S} = [\text{Re}\sum_{\mathbf{G}}\mathbf{E}^*(\mathbf{G}) \times \mathbf{H}(\mathbf{G})]/2$, which determines the group velocity direction of each mode. Consider the wavevector $\mathbf{k_s} + \mathbf{G}_{lmn}$ of these modes independently at the interface between the uniform medium and the PC region, where $s = 1, 2, \ldots, 2(2L+1)(2N+1)$. At the $y = 0$ plane, all $\mathbf{k_s}$ have the same tangential components, and all tangential components of $\mathbf{k_s} + \mathbf{G}_{lmn}$ have no $\mathbf{b}_2$ included since $\mathbf{b}_2$ is along $\hat{y}$-axis. Therefore, the wavevectors of the only allowed reflection modes at the incident side are given by

$$\begin{cases} \mathbf{k}_{ln} = k_{lnx}\hat{x} + k_{lny}\hat{y} + k_{lnz}\hat{z} \\ k_{lnx} = k_{0x} + l\cdot b_{1x} + n\cdot b_{3x} \\ k_{lnz} = k_{0z} + l\cdot b_{1z} + n\cdot b_{3z} \\ k_{lny} = -\sqrt{k_0^2 - k_{lnx}^2 - k_{lnz}^2} \end{cases}, -L \le l \le L, -N \le n \le N.$$

The EM fields at both sides of the interface can be written as

$$\begin{aligned}
E_{x,I}(\mathbf{x}) &= E_{0x}e^{i\mathbf{k}_0\cdot\mathbf{x}} + \sum_{ln} R_{lnx}e^{i\mathbf{k}_{ln}\cdot\mathbf{x}} \\
E_{z,I}(\mathbf{x}) &= E_{0z}e^{i\mathbf{k}_0\cdot\mathbf{x}} + \sum_{ln} R_{lnz}e^{i\mathbf{k}_{ln}\cdot\mathbf{x}} \\
H_{x,I}(\mathbf{x}) &= H_{0x}e^{i\mathbf{k}_0\cdot\mathbf{x}} + \sum_{ln} S_{lnx}e^{i\mathbf{k}_{ln}\cdot\mathbf{x}} \\
H_{z,I}(\mathbf{x}) &= H_{0z}e^{i\mathbf{k}_0\cdot\mathbf{x}} + \sum_{ln} S_{lnz}e^{i\mathbf{k}_{ln}\cdot\mathbf{x}} \\
E_{x,II}(\mathbf{x}) &= \sum_s\sum_{lmn} T_s E_x(s,\mathbf{G}_{lmn}) \\
&\qquad \cdot e^{i(\mathbf{k_s}+l\cdot\mathbf{b_1}+m\cdot\mathbf{b_2}+n\cdot\mathbf{b_3})\cdot\mathbf{x}} \\
E_{z,II}(\mathbf{x}) &= \sum_s\sum_{lmn} T_s E_z(s,\mathbf{G}_{lmn}) \\
&\qquad \cdot e^{i(\mathbf{k_s}+l\cdot\mathbf{b_1}+m\cdot\mathbf{b_2}+n\cdot\mathbf{b_3})\cdot\mathbf{x}} \\
H_{x,II}(\mathbf{x}) &= \sum_s\sum_{lmn} T_s H_x(s,\mathbf{G}_{lmn}) \\
&\qquad \cdot e^{i(\mathbf{k_s}+l\cdot\mathbf{b_1}+m\cdot\mathbf{b_2}+n\cdot\mathbf{b_3})\cdot\mathbf{x}} \\
H_{z,II}(\mathbf{x}) &= \sum_s\sum_{lmn} T_s H_z(s,\mathbf{G}_{lmn}) \\
&\qquad \cdot e^{i(\mathbf{k_s}+l\cdot\mathbf{b_1}+m\cdot\mathbf{b_2}+n\cdot\mathbf{b_3})\cdot\mathbf{x}} \quad (4)
\end{aligned}$$

where R_{ln} and S_{ln} are the EM field amplitudes of the reflection mode (ln) in region I. In the uniform medium, the relationship between R_{ln} and S_{ln} is given by

$$\begin{cases} S_{lnx} = \left[\left(k_0^2 - k_{lnx}^2\right)R_{lnz} + k_{lnx}k_{lnz}R_{lnx}\right]/(\omega\mu_0 k_{lny}) \\ S_{lnz} = \left[-\left(k_0^2 - k_{lnz}^2\right)R_{lnx} - k_{lnx}k_{lnz}R_{lnz}\right]/(\omega\mu_0 k_{lny}) \end{cases}. \quad (5)$$

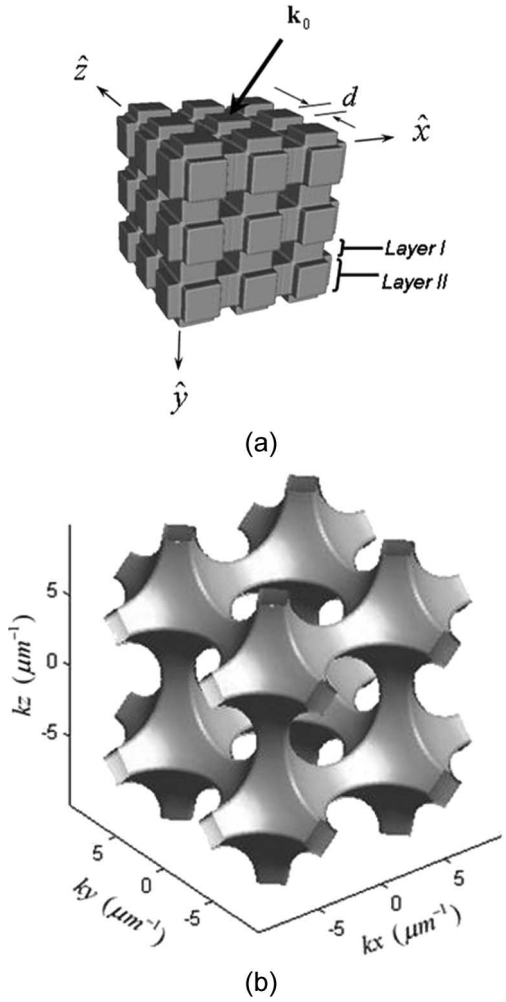

Fig. 2. (a) Schematic of a 3-D square-rod structure. (b) 3-D dispersion surface of the lowest band for the square-rod structure with $a/\lambda = 0.40$.

T_s is the amplitude of the transmission modes in region II. At the $y = 0$ plane, the distinct modes in regions I and II both reduce to $2(2L + 1)(2N + 1)$ such that the mode field amplitudes R_{lnx}, R_{lnz}, and T_s may be solved from the boundary equations.

III. Results and Discussion

To clarify the theory with an example, we assume that the PC region under consideration here is composed of polymer-based crossing square rods [9], [10] that are embedded in an air background. The index contrast is 1.5 : 1. Here, we will demonstrate how to employ our method to choose proper parameters and simulate the optical features of low-index-contrast-based PC structures. Our interest in low-index-contrast PC structures stems from a wide variety of easy and inexpensive fabrication techniques that are available for such structures, including self-assembly [11], holography [12], two-photon absorption [13], and nanoimprint [14]. Our aim is to design a 3-D PC structure exhibiting the superprism effect around the optical communication wavelengths of 1550 nm. A $3 \times 3 \times 3$ section of a general square-rod structure is depicted in Fig. 2(a). From a fabrication point of view, only two types of layers compose

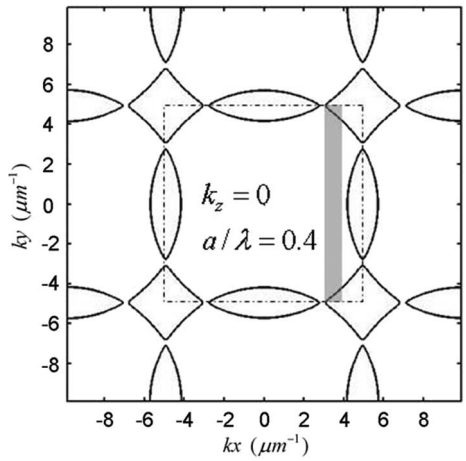

Fig. 3. Dispersion contours of all covered bands in $k_z = 0$ plane with normalized frequency of $a/\lambda = 0.4$. The first Brillouin zone is marked by a square frame.

one period, except the top and bottom ones. Thus, it is convenient for fabrication. We set the side length of the square rod $d = 0.8a$ to achieve high structure strength after fabrication. The interface between a PC and the air is (100). We have used the conventional PWE method to solve the 3-D dispersion surface of the lowest band, and the result is plotted in Fig. 2(b). The superprism effect that is caused by PC structures is usually an incidental phenomenon in a high-dispersion region. In the cross section of the dispersion surface with parallel planes, high dispersion happens around the rhombic profiles. Hereby, we may choose $k_z = k_{0z} = 0$ for simplicity.

The general PWE method is widely employed to calculate the normalized frequency a/λ of each photonic band. Then, the dispersion surface of each band for an exact frequency can be solved by interpolation. Our center of attention is the dispersion contour at several frequency points, by which we can choose a high-dispersion region and evaluate the group velocity direction. However, for the general PWE method, we must find all the bands that have common boundaries with the exact frequency. Our method is to find all k_y solutions based on the given frequencies and tangential components of the incident fields. Therefore, the dispersion contour, which is composed of all these common boundaries, can be solved simultaneously. The dispersion surface sections of the square-rod structure, which are computed by our method for three frequency points at the $k_z = 0$ plane, are plotted in Figs. 3–5. The rhombic profiles are part of the lowest band dispersion surface, which is consistent with the conventional PWE [5] calculation result shown in Fig. 2(b). Other curves are common boundaries with higher bands. The rhombic profiles actually include two similar dispersion contours for transverse-electric-like and transverse-magnetic-like modes, respectively, which exhibit similar optical properties due to the rotation symmetry of square-rod structures. We assume that the incident plane wave is a TE wave (electric field $\mathbf{E}_I$ is perpendicular to the $x - y$ plane) and only consider the dispersion contour for TE-like modes during structure parameter design. The gray areas in Figs. 3 and 4 covering the high-dispersion region only have intersections with the lowest band dispersion contour. No intersection with

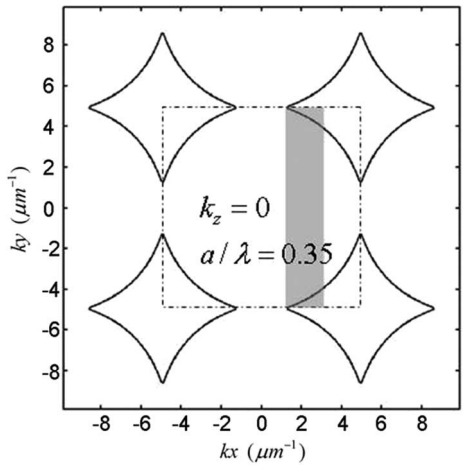

Fig. 4. Dispersion contours in the $k_z = 0$ plane with $a/\lambda = 0.35$.

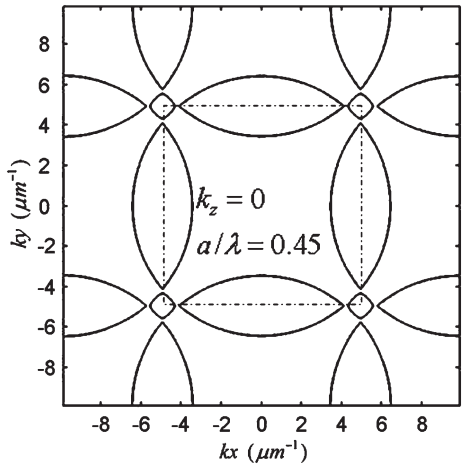

Fig. 5. Dispersion contours in the $k_z = 0$ plane with $a/\lambda = 0.45$.

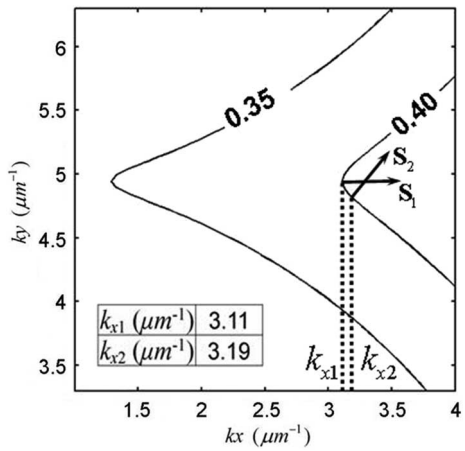

Fig. 6. Magnified dispersion contour corner of the lowest band with different normalized frequencies of $a/\lambda = 0.35$ and 0.40. The Poynting vectors $\mathbf{S_1}$ and $\mathbf{S_2}$ are marked with arrows.

a higher band implies that the structures have more chances of achieving high transmission. Thus, k_x may be adjusted within the gray areas. The high-dispersion regions in both Figs. 3 and 4 are magnified and plotted in Fig. 6, which may be used

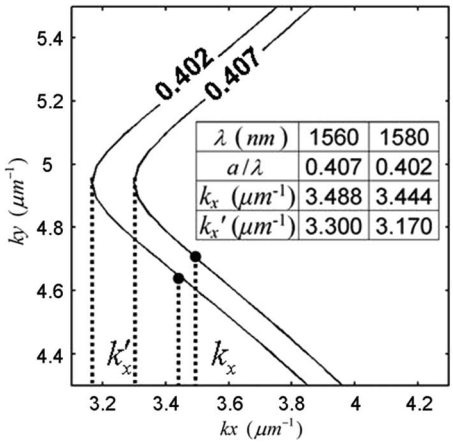

Fig. 7. Dispersion contours with 20-nm wavelength difference. The derived wavevector and contour corner position are marked as k_x and k_x', respectively. Numerical results are listed in the inset tables.

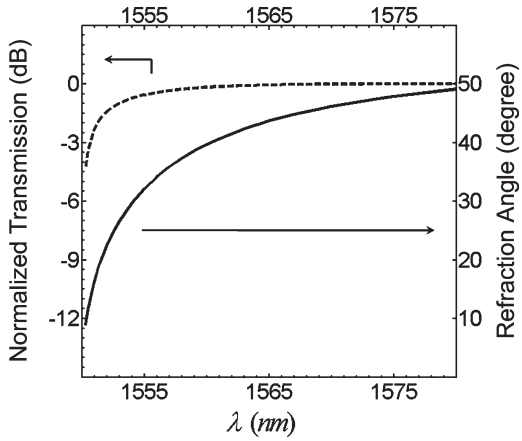

Fig. 8. Superprism effect at the lowest band of the 3-D square-rod PC. The refraction angle (solid curve) and normalized transmission (dotted curve) for the designed wavelength range (1550–1580 nm) are indicated, respectively.

to estimate the power flow direction of transmitted modes since the group velocity is perpendicular to the dispersion contour. The arrows in Fig. 6 show that a small k_x change can result in close to 45° refraction angle scanning for both frequencies, whereas the flatness difference around the contour corner is obvious. Therefore, we have chosen $a/\lambda = 0.40$ as our working frequency to achieve a smooth angular change.

Fig. 7 shows adjacent dispersion contours with a 20-nm wavelength difference, where k_x' is the apex of the contour corner. The incident angle is set at 60° to keep k_x moving around the high-dispersion region. Calculation shows that both the dispersion contour and k_x shift to the left when wavelength becomes longer, whereas the shift distances are different. The incident angle in our example has been finely adjusted to 55.8° to achieve the superprism effect in this region. The scanning effect of the refraction angle and the normalized transmission are illustrated in Fig. 8. The angular scanning range and high transmission in the designed wavelength range (1550–1580 nm) are consistent with our anticipation. The near-100% transmission proves that the PC structures behave differently from the homogeneous medium when λ is far away from the

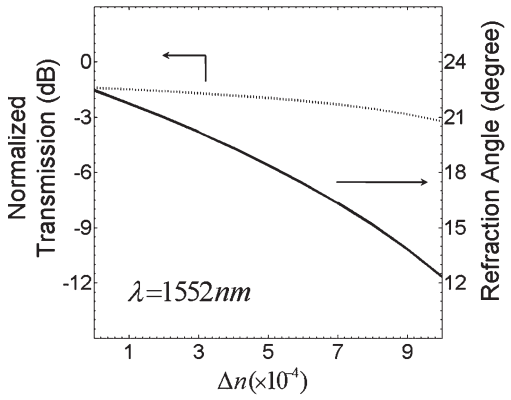

Fig. 9. Refraction angle (solid curve) and normalized transmission (dotted curve) for a PC with polymer index changed by up to 10^{-3}.

long-wavelength limit [10]. Fig. 9 indicates that the refraction angle and transmission for similar PC structures with a polymer index changed by as much as 10^{-3}, and 10° angular coverage can be achieved at $\lambda = 1552$ nm, which confirmed another feature of the superprism effect—high sensitivity to the refractive index [3]. Our theory predicts that such sensitivity is accompanied by a less than 3-dB transmission loss. Therefore, these structures are highly useful for active laser beam scanning applications, where the laser beam direction can be widely manipulated by the slight tuning of the refractive index. A total of 729 planar waves have been applied to achieve reasonable accuracy in our calculation, and the numerical stability has been verified based on energy conservation and solution convergence. By using TMM, Minami *et al.* also studied the intensity of transmitted and reflected modes in similar square-rod structures [10]. As he pointed out, the eigenvalue solutions of TMM are actually $e^{ik_y(s)d}$ which may stretch over a very large scale and result in overflow or underflow during the numerical evaluation. In contrast, our method solves $k_y(s)$ directly and keeps the numerical distribution of the solved eigenvalues within a comparatively smaller range.

IV. Conclusion

A rigorous vector-field theory has been developed to study the anomalous light refraction effect at the interface between a semi-infinite 3-D PC and a homogeneous medium. The light beam direction and optical-field amplitude of both reflected and transmitted modes through PCs are rigorously analyzed and derived as linear equations in matrix form. We have further illustrated how to employ our refraction theory on parameter adjustment to achieve the superprism effect by low-index-contrast square-rod structures. Our method can be applied to high-index-contrast PC structures as well [15]–[17]. In addition, further extending this method to disordered PCs could be another direction to explore [18].

Acknowledgment

The authors would like to thank R. L. Nelson and J. W. Haus for their helpful discussions.

References

[1] H. Kosaka, T. Kawashima, A. Tomita, M. Notomi, T. Tamamura, T. Sato, and S. Kawakami, "Superprism phenomena in photonic crystals," *Phys. Rev. B, Condens. Matter*, vol. 58, no. 16, pp. R10 096–R10 099, Oct. 1998.

[2] J. Shin and S. Fan, "Conditions for self-collimation in three-dimensional photonic crystals," *Opt. Lett.*, vol. 30, no. 18, pp. 2397–2399, Sep. 2005.

[3] T. Prasad, V. Colvin, and D. Mittleman, "Superprism phenomenon in three-dimensional macroporous polymer photonic crystals," *Phys. Rev. B, Condens. Matter*, vol. 67, no. 16, p. 165 103, Apr. 2003.

[4] Z. Lu, J. A. Murakowski, C. A. Schuetz, S. Shi, G. J. Schneider, and D. W. Prather, "Three-dimensional subwavelength imaging by a photonic-crystal flat lens using negative refraction at microwave frequencies," *Phys. Rev. Lett.*, vol. 95, no. 15, p. 153 901, Oct. 2005.

[5] S. G. Johnson and J. D. Joannopoulos, "Block-iterative frequency-domain methods for Maxwell's equations in a planewave basis," *Opt. Express*, vol. 8, no. 3, pp. 173–190, Jan. 2001.

[6] Z. Li and K. Ho, "Application of structural symmetries in the plane-wave-based transfer-matrix method for three-dimensional photonic crystal waveguides," *Phys. Rev. B, Condens. Matter*, vol. 68, no. 24, p. 155 101, Dec. 2003.

[7] W. Jiang, R. T. Chen, and X. Lu, "Theory of light refraction at the surface of a photonic crystal," *Phys. Rev. B, Condens. Matter*, vol. 71, no. 24, p. 245 115, Jun. 2005.

[8] W. Jiang and R. T. Chen, "Rigorous analysis of diffraction gratings of arbitrary profiles using virtual photonic crystals," *J. Opt. Soc. Amer. A, Opt. Image Sci.*, vol. 23, no. 9, pp. 2192–2197, Sep. 2006.

[9] H. S. Sozuer and J. W. Haus, "Photonic bands—Simple-cubic lattice," *J. Opt. Soc. Amer. B, Opt. Phys.*, vol. 10, no. 2, pp. 296–302, Feb. 1993.

[10] T. Minami, H. Ajiki, and K. Cho, "Branching ratio of light incident on a photonic crystal in a multibranch dispersion region," *Physica E—Low-Dimensional Systems Nanostructures*, vol. 13, no. 2–4, pp. 432–436, Mar. 2002.

[11] Y. A. Vlasov, X.-Z. Bo, J. C. Sturm, and D. J. Norris, "On-chip natural assembly of silicon photonic bandgap crystals," *Nature*, vol. 414, no. 6861, pp. 289–293, Nov. 2001.

[12] J. Chen, W. Jiang, X. Chen, L. Wang, S. Zhang, and R. T. Chen, "Holographic three-dimensional polymeric photonic crystals operating in the 1550 nm window," *Appl. Phys. Lett.*, vol. 90, no. 9, p. 093 102, Feb. 2007.

[13] V. Mizeikis, K. K. Seet, S. Juodkazis, and H. Misawa, "Three-dimensional woodpile photonic crystal templates for the infrared spectral range," *Opt. Lett.*, vol. 29, no. 17, pp. 2061–2063, Sep. 2004.

[14] K. Inoue and K. Ohtaka, *Photonic Crystals: Physics, Fabrication and Applications*. New York: Springer-Verlag, 2004.

[15] L. Gu, W. Jiang, X. Chen, L. Wang, and R. T. Chen, "High speed silicon photonic crystal waveguide modulator for low voltage operation," *Appl. Phys. Lett.*, vol. 90, no. 7, p. 071 105, Feb. 2007.

[16] L. Gu, W. Jiang, X. Chen, and R. T. Chen, "Thermooptically tuned photonic crystal waveguide silicon-on-insulator Mach–Zehnder interferometers," *IEEE Photon. Technol. Lett.*, vol. 19, no. 5, pp. 342–344, Mar. 2007.

[17] Y. Jiang, W. Jiang, L. Gu, X. Chen, and R. T. Chen, "80-micron interaction length silicon photonic crystal waveguide modulator," *Appl. Phys. Lett.*, vol. 87, no. 22, p. 221 105, Nov. 2005.

[18] W. Jiang and C. Gong, "Two mechanisms, three stages of the localization of light in a disordered dielectric structure with photonic band gaps," *Phys. Rev. B, Condens. Matter*, vol. 60, no. 17, p. 12 015, Nov. 1999.

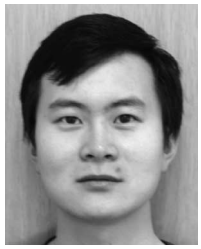

Xiaonan Chen received the B.S. degree in precision instruments and mechanology from Tsinghua University, Beijing, China, and the M.S. degree in electrical and computer engineering from the University of Texas at Austin. He is currently working toward the Ph.D. degree with the Microelectronics Research Center, University of Texas at Austin.

From 2003 to 2005, his research topic was polymeric photonic devices for true time delay optical interconnects. His current research includes photonic crystals and silicon photonics.

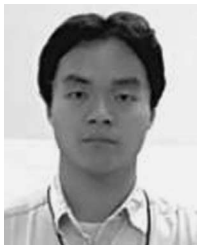

Wei Jiang (M'05) received the B.S. degree in physics from Nanjing University, Nanjing, China, and the M.A. degree in physics and the Ph.D. degree in electrical and computer engineering from the University of Texas at Austin.

In 2001, he was with Radiant Photonics, where he developed a ball-lens optical add-drop multiplexer for wavelength division multiplexing applications. Since 2004, he has been with Omega Optics, Inc., Austin, where he is currently a Senior Research Scientist. He is also with the Microelectronics Research Center, University of Texas at Austin. His research interests encompass photonic crystals, silicon photonics, nanoimprints, fiber optics, and optical interconnects.

Dr. Jiang is a member of the International Society for Optical Engineers, the Optical Society of America, and Tau Beta Pi Engineering Honor Society.

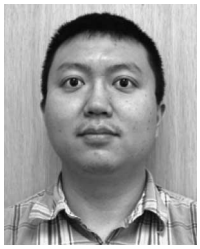

Jiaqi Chen received the B.S. degree in electronic engineering from Tsinghua University, Beijing, China, in 2004 and the M.S. degree in electrical and computer engineering from the University of Texas at Austin in 2007.

He is currently with the Microelectronics Research Center, University of Texas at Austin. His current research interests include nanophotonics, holography, and photonic crystals.

Mr. Chen is a member of the International Society for Optical Engineers.

Ray T. Chen (F'04) received the B.S. degree in physics from the National Tsing Hua University, Hsinchu, Taiwan, R.O.C., in 1980, the M.S. degree in physics from the University of California, Irvine, in 1983, and the Ph.D. degree in electrical engineering from the University of California, San Diego, in 1988.

From 1988 to 1992, he was a Research Scientist, a Manager, and the Director of the Department of Electrooptic Engineering, Physical Optics Corporation, Torrance, CA. He joined the University of Texas at Austin (UT Austin) in 1992 as a member of the faculty of the Electrical and Computer Engineering Department, where he started an optical interconnect research program and is currently the Cullen Trust for Higher Education Endowed Professor and the Director of the Nanophotonics and Optical Interconnect Research Laboratory, Microelectronics Research Center. He was the Chief Technical Officer/Founder and Chairman of the Board of Radiant Research from 2000 to 2001, where he raised $18 million A-Round funding to commercialize polymer-based photonic devices. He was also the Founder and Chairman of the Board of Omega Optics, Inc., since its inception in 2001. He has been a Consultant for various federal agencies and private companies and has delivered numerous invited talks to professional societies. He has served as the Editor or a Coeditor of 18 conference proceedings. His group at UT Austin has reported its research findings in more than 440 published papers, including over 60 invited papers with over 1400 citations according to Google Scholar Search. He is the holder of 17 issued patents. His research interests include nanophotonic passive and active devices for optical interconnect applications, polymer-based guided-wave optical interconnection and packaging, and true-time-delay wideband phased array antenna. Experiences garnered through these programs in polymeric material processing and device integration are pivotal elements for the research work conducted by his group.

Dr. Chen is a Fellow of the Optical Society of America (OSA) and the International Society of Optical Engineering (SPIE). He is the recipient of 84 research grants and contracts from such sponsors as the Department of Defense, the National Science Foundation, the Department of Energy, the National Aeronautics and Space Administration, the State of Texas, and private industry. He was the recipient of the 1987 University of California Regent's Dissertation Fellowship and the 1999 UT Engineering Foundation Faculty Award for his contributions in research, teaching, and services. During undergraduate years with the National Tsing Hua University, he led a university debate team that won the national debate contest national championship in Taiwan in 1979. He was the Chair or a Program Committee Member for more than 60 domestic and international conferences organized by the IEEE, SPIE, OSA, and the Photonics Society of Chinese Americans.